MODELING AND SIMULATION OF AMPEROMETRIC BIOSENSORS ACTING IN FLOW INJECTION ANALYSIS

Romas Baronas[a], Darius Baronas[b]
[a]Department of Software Engineering, Vilnius University, Didlaukio str. 47, LT-08303, Vilnius, Lithuania
[b]Institute of Mathematics and Informatics, Vilnius University, Akademijos str. 4, LT-08663, Vilnius, Lithuania
Emails: [a]romas.baronas@mif.vu.lt, [b]darius.baronas@mif.vu.lt

ABSTRACT
This paper deals with amperometric biosensors acting in the flow injection mode when the biosensor contacts with an analyte for a short time. A biosensor-based analytical system is mathematically modeled by reaction-diffusion equations containing a non-linear term related to the Michaelis-Menten kinetics of an enzymatic reaction. The model involves four regions: the enzyme layer where enzymatic reaction as well as the mass transport by diffusion take place, a dialysis membrane and a diffusion limiting region where only the diffusion take place, and a convective region where the analyte concentration is maintained constant. The system of equations was solved numerically by using the finite difference technique. The biosensor operation is analyzed with a special emphasis to the effect of the dialysis membrane on the biosensor response. The biosensor sensitivity is investigated by altering the model parameters influencing the thickness of the dialysis membrane and the catalytic activity of the enzyme. The half maximal effective concentration of the analyte is used as a main characteristic of the sensitivity and the calibration curve of the biosensor.

Keywords: modeling, reaction-diffusion, biosensor, flow injection analysis.

1. INTRODUCTION
Biosensors are analytical devices mainly used for measuring concentrations of analytes (substrates). Main parts composing a biosensor, a biologically active substance, usually an enzyme, and a physicochemical transducer are combined to convert a biochemical reaction result to a measurable quantity (Gutfreund 1995; Turner et al. 1990; Scheller and Schubert 1992). Amperometric biosensors measure changes in the current on the working electrode due to the direct oxidation or reduction of chemical reaction products. The measured current is usually proportional to the concentration of the analyte (substrate). The amperometric biosensors are relatively cheap, sensitive and reliable devices for clinical diagnostics, drug detection, food analysis and environment monitoring (Wollenberger et al. 1997; Gruhl et al. 2011; Viswanathan et al. 2009).

Amperometric biosensors are rather often combined with the flow injection analysis (FIA) for on-line monitoring of raw materials, product quality and the manufacturing process (Ruzicka and Hansen 1988; Mello and Kubota 2002; Nenkova et al. 2010). In the FIA a biosensor contacts with the substrate for short time (seconds to tens of seconds) whereas in the batch analysis the biosensor remains immersed in the substrate solution for a long time (Ruzicka and Hansen 1988). Compared to the batch systems, the FIA systems present the advantages of the reduction in analysis time allowing a high sample throughput, and the possibility to work with small volumes of the substrate (Prieto-Simon et al. 2006; Hernandez et al. 2013). The FIA arrangement also presents a wide response range and high sensitivity (Prieto-Simon et al. 2006).

To improve the efficiency of the development of a novel biosensor as well as to optimize its configuration it is of crucial important to model the biosensor action (Bartlett and Whitaker 1987; Schulmeister 1990; Amatore et al. 2006; Lyons 2009). Biosensors acting in the FIA mode have been already modeled usually at internal diffusion limitations by ignoring the external diffusion (Zhang et al. 2001; Baronas et al. 2002). However, in practical biosensing systems, the mass transport outside the enzyme region is of crucial importance, and it has to be taken into consideration when modeling the biosensor action (Lyons 2009). Recently, the mechanisms controlling the sensitivity of amperometric biosensors acting in FIA mode were numerically modeled taking into consideration the external mass transport (Baronas et al. 2011). The mass transport by diffusion is especially important when dialysis membranes are applied for development of highly stable and sensitive biosensors (Baronas et al. 2010).

The goal of this investigation was to develop a computational model for an effective simulation of the action of an amperometric biosensor containing a dialysis membranes and utilizing FIA as well as to investigate the influence of the physical and kinetic parameters on the biosensor response. The biosensing system was mathematically modeled by reaction-diffusion equations containing a non-linear term related to the Michaelis-Menten kinetics of an enzymatic reaction (Bartlett and Whitaker 1987; Schulmeister 1990). The system of equations was solved numerically by using the finite difference technique (Baronas et al. 2010; Britz 2005). The biosensor

operation was analyzed with a special emphasis to the effect of the dialysis membrane on the biosensor response. The biosensor sensitivity was investigated by altering the model parameters influencing the thickness of the dialysis membrane and the catalytic activity of the enzyme. The half maximal effective concentration of the analyte was used as a main characteristic of the sensitivity and the calibration curve of the biosensor (Bisswanger 2008).

2. BIOSENSOR STRUCTURE

The biosensor to be modeled has a layered structure (Simelevicius et al. 2012). Figure 1 shows a principal structure of the biosensor. The biosensor is considered as an electrode with a relatively thin layer of an enzyme (enzyme membrane) entrapped on the surface of the electrode by applying a dialysis membrane. The biosensor model involves four regions: the enzyme layer where the enzyme reaction as well as the mass transport by diffusion take place, a dialysis membrane and a diffusion limiting region where only the mass transport by diffusion take place, and a convective region where the analyte concentration is maintained constant.

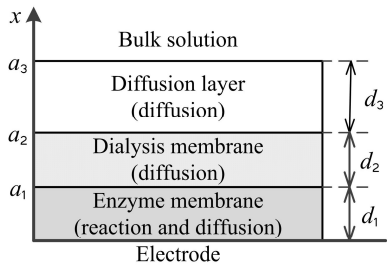

Figure 1: Structural Scheme of the Biosensor

In the enzyme layer we consider the enzyme-catalyzed reaction

$$\mathrm{E} + \mathrm{S} \underset{k_{-1}}{\overset{k_1}{\rightleftharpoons}} \mathrm{ES} \xrightarrow{k_2} \mathrm{E} + \mathrm{P}, \tag{1}$$

where the substrate (S) combines reversibly with an enzyme (E) to form a complex (ES). The complex then dissociates into the product (P) and the enzyme is regenerated (Gutfreund 1995; Scheller and Schubert 1992).

Assuming the quasi steady-state approximation, the concentration of the intermediate complex (ES) does not change and may be neglected when modeling the biochemical behavior of biosensors (Turner et al. 1990; Scheller and Schubert 1992; Segel and Slemrod 1989). In the resulting scheme, the substrate (S) is enzymatically converted to the product (P),

$$\mathrm{S} \xrightarrow{\mathrm{E}} \mathrm{P} \tag{2}$$

It was assumed that $x = 0$ represents the surface of the electrode, a_1, a_2 and a_3 denote the distances from the electrode surface, while d_1, d_2 and d_3 are the thicknesses of the enzyme, the dialysis membrane and the diffusion layers, respectively, $a_i = a_{i-1} + d_i$, $i = 1, 2, 3$, and $a_0 = 0$. The outer diffusion layer ($a_2 < x < a_3$) may be treated as the Nernst diffusion layer (Britz 2005). According to the Nernst approach a layer of thickness d_3 = $a_3 - a_2$ remains unchanged with time. It was assumed that away from it the buffer solution is uniform in concentration.

3. MATHEMATICAL MODEL

Assuming a homogeneous distribution of the enzyme in the enzyme layer of the uniform thickness and symmetrical geometry of the dialysis membrane leads to the mathematical model of the biosensor action defined in a one-dimensional-in-space domain (Schulmeister 1990; Baronas et al. 2010).

3.1. Governing equations

Coupling the enzyme-catalyzed reaction (2) in the enzyme layer with the mass transport by diffusion, described by Fick's law, leads to the following system of the reaction-diffusion equations ($t > 0$):

$$\frac{\partial S_1}{\partial t} = D_{S_1} \frac{\partial^2 S_1}{\partial x^2} - \frac{V_{\max} S_1}{K_M + S_1}, \tag{3a}$$

$$\frac{\partial P_1}{\partial t} = D_{P_1} \frac{\partial^2 P_1}{\partial x^2} + \frac{V_{\max} S_1}{K_M + S_1}, \quad x \in (0, a_1), \tag{3b}$$

where x and t stand for space and time, S_1 and P_1 are the concentrations of the substrate (S) and the product (P) in the enzyme layer, D_{S_1}, D_{P_1} are the constant diffusion coefficients, $V_{\max}$ is the maximal enzymatic rate attainable with that amount of the enzyme, when the enzyme is fully saturated with the substrate, K_M is the Michaelis constant, and $d_1 = a_1$ is the thickness of the enzyme layer (Kulys 1981; Bartlett and Whitaker 1987; Schulmeister 1990). The Michaelis constant K_M is the concentration of the substrate (S) at which the reaction rate is half its maximum value $V_{\max}$. K_M is an approximation of the enzyme affinity for the substrate based on the rate constants within the reactions (1), $K_M = (k_{-1} + k_2)/k_1$.

Outside the enzyme layer, only the mass transport by diffusion of the substrate as well as the product takes place ($t > 0$),

$$\frac{\partial S_i}{\partial t} = D_{S_i} \frac{\partial^2 S_i}{\partial x^2}, \tag{4a}$$

$$\frac{\partial P_i}{\partial t} = D_{P_i} \frac{\partial^2 P_i}{\partial x^2}, \quad x \in (a_{i-1}, a_i),\ i = 2, 3, \tag{4b}$$

where S_i and P_i are the substrate and the product concentrations in the i-th layer, D_{S_i} and D_{P_i} are the diffusion coefficients, and $d_i = a_i - a_{i-1}$ is the thickness of the corresponding layer, $i = 2, 3$.

3.2. Initial conditions

The biosensor operation starts when the substrate appears in the bulk solution. This leads to the following

initial conditions ($t = 0$):

$$S_1(x,0) = 0, \quad P_1(x,0) = 0, \quad x \in [0, a_1], \tag{5a}$$

$$S_2(x,0) = 0, \quad P_2(x,0) = 0, \quad x \in [a_1, a_2], \tag{5b}$$

$$S_3(x,0) = \begin{cases} 0, & x \in [a_2, a_3), \\ S_0, & x = a_3, \end{cases} \tag{5c}$$

$$P_3(x,0) = 0, \quad x \in [a_2, a_3], \tag{5d}$$

where S_0 is the substrate concentration in the bulk solution.

3.3. Boundary conditions

During the biosensor operation, the substrate penetrates through the diffusion layer as well as the dialysis membrane and reaches farther boundary of the enzyme layer ($x = a_1$). On the boundary between two adjacent regions having different diffusivities, the matching conditions have to be defined ($t > 0, i = 1, 2$):

$$D_{S_i} \frac{\partial S_i}{\partial x}\bigg|_{x=a_i} = D_{S_{i+1}} \frac{\partial S_{i+1}}{\partial x}\bigg|_{x=a_i}, \tag{6a}$$

$$S_i(a_i, t) = S_{i+1}(a_i, t), \tag{6b}$$

$$D_{P_i} \frac{\partial P_i}{\partial x}\bigg|_{x=a_i} = D_{P_{i+1}} \frac{\partial P_{i+1}}{\partial x}\bigg|_{x=a_i}, \tag{6c}$$

$$P_i(a_i, t) = P_{i+1}(a_i, t). \tag{6d}$$

These conditions mean that fluxes of the substrate and the product through one region are equal to the corresponding fluxes entering the surface of the neighboring region. Concentrations of the substrate and the product in one region versus the neighboring region are assumed to be equal.

Due to the electrode polarization the concentration of the reaction product at the electrode surface is permanently reduced to zero (Schulmeister 1990; Baronas et al. 2010),

$$P_1(0, t) = 0. \tag{7}$$

Due to the substrate electro-inactivity, the substrate concentration flux on the electrode surface equals zero,

$$\frac{\partial S_1}{\partial x}\bigg|_{x=0} = 0. \tag{8}$$

According to the Nernst approach the layer of the thickness d_3 of the outer diffusion layer remains unchanged with time, and away from it the solution is uniform in the concentration (Britz 2005). In the FIA mode of the biosensor operation, the substrate appears in the bulk solution only for a short time period called the injection time (Ruzicka and Hansen 1988). Later, the substrate disappears from the bulk solution,

$$P_3(a_3, t) = 0, \quad t > 0, \tag{9a}$$

$$S_3(a_3, t) = \begin{cases} S_0, & 0 < t \le T_F, \\ 0, & t > T_F, \end{cases} \tag{9b}$$

where T_F is the injection time.

3.4. Biosensor response

The anodic or cathodic current is measured as a result in a physical experiment. The biosensor current is proportional to the gradient of the reaction product concentration at the electrode surface, i.e. on the boundary $x = 0$. When modeling the biosensor action, due to the direct proportionality of the current to the area of the electrode surface, the current is often normalized with that area (Schulmeister 1990; Baronas et al. 2010). The density $I(t)$ of the biosensor current at time t can be obtained explicitly from Faraday's and Fick's laws (Schulmeister 1990),

$$I(t) = n_e F D_{P_1} \frac{\partial P_1}{\partial x}\bigg|_{x=0}, \tag{10}$$

where n_e is a number of electrons involved in a charge transfer, and F is the Faraday constant.

We assume that the system reaches equilibrium when $t \to \infty$. The steady-state current is usually assumed to be the main characteristic of commercial amperometric biosensors acting in the batch mode (Gutfreund 1995; Turner et al. 1990; Scheller and Schubert 1992). In the FIA, due to the zero concentration of the surrounding substrate at $t > T_F$, the steady-state current falls to zero, $I(t) \to 0$, when $t \to \infty$. Because of this, the maximum peak current is the mostly used characteristic in FIA systems,

$$I_{\max} = \max_{t>0} \{I(t)\}, \tag{11}$$

where $I_{\max}$ is the maximal density of the biosensor current.

The corresponding time $T_{\max}$ of the maximal current is used to characterize the response time of the biosensor,

$$T_{\max} = \{t : I(t) = I_{\max}\}. \tag{12}$$

3.5. Characteristics of Biosensor Response

The sensitivity is one of the most important characteristics of the biosensor operation (Gutfreund 1995; Turner et al. 1990; Scheller and Schubert 1992). The sensitivity B_S of the biosensor acting in the FIA mode is defined as the gradient of the maximal current with respect to the concentration S_0 of the substrate in the bulk (Schulmeister 1990; Baronas et al. 2010). Since the biosensor current as well as the substrate concentration vary even in orders of magnitude, a dimensionless expression of the sensitivity is preferable (Baronas et al. 2010). The dimensionless sensitivity $B_S(S_0)$ for the substrate concentration S_0 is given by

$$B_S(S_0) = \frac{\mathrm{d}I_{\max}(S_0)}{\mathrm{d}S_0} \times \frac{S_0}{I_{\max}(S_0)}, \tag{13}$$

where $I_{\max}(S_0)$ is the density of the maximal biosensor current calculated at the substrate concentration S_0.

In the Michaelis-Menten kinetic model, the Michaelis constant K_M as a characteristic of the biosensor calibration curve is numerically equal to the substrate concentration at which half the maximum rate of the enzyme-catalyzed reaction is achieved (Gutfreund 1995; Scheller and Schubert 1992). Under certain conditions, especially under diffusion limitations for the substrate, the half maximal effective concentration C_{50} of the substrate to be determined is often used to characterize the biosensor calibration curve (Bisswanger 2008). In the case of FIA analysis, C_{50} is defined as the concentration of the substrate at which the response of the biosensor reaches half of the maximal response,

$$C_{50} = \left\{ S_0^* : I_{\max}(S_0^*) = 0.5 \lim_{S_0 \to \infty} I_{\max}(S_0) \right\}, \quad (14)$$

where $I_{\max}(S_0)$ is the maximal density of the biosensor current calculated at the substrate concentration S_0.

A greater value of the half maximal effective concentration C_{50} corresponds to a longer linear part of the calibration curve (Bisswanger 2008). At the substrate concentration S_0 corresponding to a linear part of the calibration curve ($S_0 < C_{50}$) the dimensionless biosensor sensitivity $B_S(S_0)$ is approximately equal to unity (Baronas et al. 2010). The concentration C_{50} well characterizes the overall sensitivity of the biosensor.

In the case of biosensors acting in batch mode and exhibiting the Michaelis-Menten kinetics, the concentration C_{50} is usually called the apparent Michaelis-Menten constant (Stikoniene et al. 2010). It has been shown that, under certain conditions, the apparent Michaelis constant highly depends on the biosensor geometry (Ivanauskas et al. 2008). Also, a substantial increase of the apparent Michaelis constant has been shown at restricted diffusion of the substrate through an outer membrane covering an enzyme layer (Stikoniene et al. 2010). This result appears to be of a high practical interest, since it enables to expand the linear dependence of biosensor response on the substrate concentration towards the higher concentrations under the deep diffusion mode of the biosensor operation, whereas the response time increases not very drastic (Stikoniene et al. 2010). This property is especially attractive for biosensors acting in FIA mode because of a relatively short their response time (Cervini and Cavalheiro 2008; Baronas et al. 2002).

3.6. Dimensionless Model

In order to extract the main governing parameters of the mathematical model, thus reducing a number of model parameters in general, a dimensionless model is often derived (Amatore et al. 2006; Schulmeister 1990). The dimensionless model has been derived by replacing the model parameters as defined in Table 1.

For the enzyme layer, the reaction-diffusion equations (3) can be rewritten as follows ($\hat{t} > 0$):

Table 1: Dimensional and Dimensionless Model Parameters ($i = 1, 2, 3$)

Dimensional	Dimensionless
x, cm	$\hat{x} = x/d_1$
a_i, cm	$\hat{a_i} = a_i/d_1$
d_i, cm	$\hat{d_i} = d_i/d_1$
t, s	$\hat{t} = tD_{S_1}/d_1^2$
T_F, s	$\hat{T_F} = T_F D_{S_1}/d_1^2$
S_i, M	$\hat{S_i} = S_i/K_M$
P_i, M	$\hat{P_i} = P_i/K_M$
C_{50}, M	$\hat{C_{50}} = C_{50}/K_M$
D_{S_i}, cm^2/s	$\hat{D}_{S_i} = D_{S_i} / D_{S_1}$
D_{P_i}, cm^2/s	$\hat{D}_{P_i} = D_{P_i} / D_{S_1}$
I, A/cm^2	$\hat{I} = Id_1/(n_e F D_{P_1} K_M)$

$$\frac{\partial \hat{S}_1}{\partial \hat{t}} = \frac{\partial^2 \hat{S}_1}{\partial \hat{x}^2} - \alpha^2 \frac{\hat{S}_1}{1 + \hat{S}_1}, \quad (15a)$$

$$\frac{\partial \hat{P}_1}{\partial \hat{t}} = \hat{D}_{P_1} \frac{\partial^2 \hat{P}_1}{\partial \hat{x}^2} + \alpha^2 \frac{\hat{S}_1}{1 + \hat{S}_1}, \quad \hat{x} \in (0, 1), \quad (15b)$$

where α^2 is the diffusion module, also known as Damköhler number (Schulmeister 1990),

$$\alpha^2 = \frac{d_1^2 V_{\max}}{D_{S_1} K_M}. \quad (16)$$

The diffusion module α^2 compares the rate of the enzyme reaction ($V_{\max}/K_M$) with the rate of the mass transport through the enzyme layer (D_{S_1}/d_1^2).

The diffusion equations (4) are transformed as follows ($\hat{t} > 0$):

$$\frac{\partial \hat{S}_i}{\partial \hat{t}} = \hat{D}_{S_i} \frac{\partial^2 \hat{S}_i}{\partial \hat{x}^2}, \quad (17a)$$

$$\frac{\partial \hat{P}_i}{\partial \hat{t}} = \hat{D}_{P_i} \frac{\partial^2 \hat{P}_i}{\partial \hat{x}^2}, \quad \hat{x} \in (\hat{a}_{i-1}, \hat{a}_i), \quad i = 2, 3. \quad (17b)$$

The initial conditions (5) take the following form ($i = 1, 2$):

$$\hat{S}_i(\hat{x}, 0) = 0, \quad \hat{P}_i(\hat{x}, 0) = 0, \quad \hat{x} \in [\hat{a}_{i-1}, \hat{a}_i], \quad (18a)$$

$$\hat{S}_3(\hat{x}, 0) = \begin{cases} 0, & \hat{x} \in [\hat{a}_2, \hat{a}_3), \\ \hat{S}_0, & \hat{x} = \hat{a}_3, \end{cases} \quad (18b)$$

$$\hat{P}_3(x, 0) = 0, \quad \hat{x} \in [\hat{a}_2, \hat{a}_3]. \quad (18c)$$

The matching conditions (6) transform to the following conditions ($\hat{t} > 0$, $i = 1, 2$):

$$\hat{D}_{S_i}\frac{\partial \hat{S}_i}{\partial \hat{x}}\bigg|_{\hat{x}=\hat{a}_i} = \hat{D}_{S_{i+1}}\frac{\partial \hat{S}_{i+1}}{\partial \hat{x}}\bigg|_{\hat{x}=\hat{a}_i}, \tag{19a}$$

$$\hat{S}_i(\hat{a}_i,\hat{t}) = \hat{S}_{i+1}(\hat{a}_i,\hat{t}), \tag{19b}$$

$$\hat{D}_{P_i}\frac{\partial \hat{P}_i}{\partial \hat{x}}\bigg|_{\hat{x}=\hat{a}_i} = \hat{D}_{P_{i+1}}\frac{\partial \hat{P}_{i+1}}{\partial \hat{x}}\bigg|_{\hat{x}=\hat{a}_i}, \tag{19c}$$

$$\hat{P}_i(\hat{a}_i,\hat{t}) = \hat{P}_{i+1}(\hat{a}_i,\hat{t}). \tag{19d}$$

The boundary conditions (7)-(9) take the following form ($\hat{t} > 0$):

$$\hat{P}_1(0,\hat{t}) = 0, \quad \frac{\partial \hat{S}_1}{\partial \hat{x}}\bigg|_{\hat{x}=0} = 0, \tag{20a}$$

$$\hat{P}_3(\hat{a}_3,\hat{t}) = 0, \tag{20b}$$

$$\hat{S}_3(\hat{a}_3,\hat{t}) = \begin{cases} \hat{S}_0, & \hat{t} \le \hat{T}_F, \\ 0, & \hat{t} > \hat{T}_F. \end{cases} \tag{20c}$$

The dimensionless current (flux) $\hat{I}$ is defined as follows:

$$\hat{I}(\hat{t}) = \frac{\partial \hat{P}_1}{\partial \hat{x}}\bigg|_{\hat{x}=0} = \frac{I(t)d_1}{n_e F D_{P_1} K_M}. \tag{21}$$

Assuming the same diffusion coefficients of the substrate and the product, the initial set of model parameters reduces to the following aggregate dimensionless parameters: $\hat{d}_2$ - the thickness of the dialysis membrane, $\hat{d}_3$ - the diffusion layer thickness, α^2 - the diffusion module, $\hat{T}_F$ - the injection time, $\hat{S}_0$ - the substrate concentration in the bulk during the injection, and $\hat{D}_{S_i} = D_{S_i}/D_{S_1} = D_{P_i}/D_{P_1} = \hat{D}_{P_i}$ - the ratio of the diffusion coefficient in the dialysis membrane (at $i = 2$) or in the diffusion layer (at $i = 3$) to the corresponding diffusion coefficient in the enzyme layer.

The diffusion module α^2 is one of the most important parameters essentially defining internal characteristics of layered amperometric biosensors (Kulys 1981; Bartlett and Whitaker 1987; Schulmeister 1990; Baronas et al. 2010). The biosensor response is known to be under diffusion control when $\alpha^2 \gg 1$. In the very opposite case, when $\alpha^2 \ll 1$, the enzyme kinetics predominates in the response.

4. NUMERICAl SIMULATION

An exact analytical solution is practically possible because of the nonlinearity of the governing equations of the mathematical model (3)-(10) (Schulmeister 1990; Kernevez 1980). Because of this the initial boundary value problem was solved numerically. Solving the problem, an implicit finite difference scheme was built on a uniform discrete grid (Schulmeister 1990; Baronas et al. 2010; Britz 2005; Britz et al. 2009). The computational model was programmed in the C language (Press et al. 1992).

The mathematical model and the numerical solution were validated using a known analytical solution (Schulmeister 1990). Assuming $T_F \to \infty$ and $d_2 \to 0$ or $d_3 \to 0$, the mathematical model (3)-(10) approaches the two compartment model of the amperometric biosensor acting in the batch mode (Schulmeister 1990). The three compartment model approaches the two compartment model also in the unrealistic case where the diffusion coefficients for the dialysis membrane are assumed to be the same as for the diffusion layer, $D_{S_2} = D_{S_3}$ and $D_{P_2} = D_{P_3}$. Additionally assuming $S_0 \ll K_M$, the nonlinear Michaelis-Menten reaction function in (3) simplifies to a linear function $V_{\max}S_1/K_M$. At these assumptions the model (3)-(10) has been solved analytically (Schulmeister 1990). At the steady-state conditions the relative difference between numerical and analytical solutions was less than 1%.

To investigate the effect of the dialysis membrane on the biosensor response, a number of experiments were carried out, while values of some parameters were kept constant (Gough and Leypoldt 1979; van Stroe-Blezen et al. 1993),

$$\begin{aligned} &K_M = 100\mu\mathrm{M}, \quad D_{S_1} = D_{P_1} = 300\,\mu\mathrm{m}^2/\mathrm{s}, \\ &D_{S_2} = D_{P_2} = 0.3D_{S_1}, \quad D_{S_3} = D_{P_3} = 2D_{S_1}, \\ &n_e = 1, \quad d_1 = 200\,\mu\mathrm{m}, \quad d_3 = 20\,\mu\mathrm{m}. \end{aligned} \tag{22}$$

To minimize the effect of the Nernst diffusion layer on the biosensor response, the responses were simulated at a practically minimal thickness ($d_3 = 20\,\mu\mathrm{m}$) of the external diffusion layer assuming well stirred buffer solution by a magnetic stirrer (Gough and Leypoldt 1979).

Figure 2 shows the evolution of the density $I(t)$ of the biosensor current simulated at a moderate concentration S_0 of the substrate ($S_0 = K_M$) and different values of the other model parameters: the maximal enzymatic rate $V_{\max}$ (0.75 and 1.5 μM), the injection time T_F (3 and 6 s) and the thickness d_2 of the dialysis membrane (10 and 20 μm). Assuming (22), these two values of the maximal enzymatic rate $V_{\max}$ correspond to the following two values of the dimensionless diffusion module α^2: 1 and 2. Accordingly, $d_2 = 10\,\mu\mathrm{m}$ corresponds to the dimensionless relative thickness $\hat{d}_2$ of the dialysis membrane equal to 0.05, while $d_2 = 20\,\mu\mathrm{m}$ leads to $\hat{d}_2 = 0.1$.

Figure 2 shows a non-monotonic behavior of the biosensor current. In all the simulated cases the current increases with increasing time t up to the injection time T_F ($t \le T_F$). However, the current also increases some time after the substrate disappearing from the bulk solution ($t \ge T_F$). The time moment $T_{\max}$ of the peak current and the peak current $I_{\max}$ depend on the model parameters: $V_{\max}$, T_F and d_2. In all the simulated cases, the time moment of the peak current was greater than T_F ($T_{\max} > T_F$).

As one can see in figure 2 that at different values of

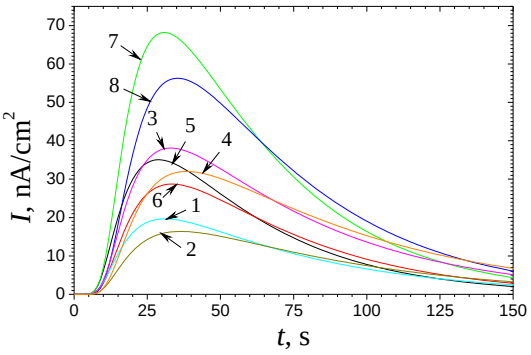

Figure 2: Dynamics of the Biosensor Response; $V_{\max}$: 0.75 (1-4), 1.5 μM (5-8), T_F: 3 (1, 2, 5, 6), 6 s (3, 4, 7, 8); d_2: 10 (1, 3, 5, 7), 20 μm (2, 4, 6, 8)

the model parameters $V_{\max}$ and d_2, the density $I_{\max}$ of the maximal current increases almost two times when the injection time T_F doubles. However, the influence of the doubling the time T_F on the time of the maximal current is rather slight. When comparing curves 1 ($T_F = 3$) and 3 ($T_F = 6\,s$) one can see that the time $T_{\max}$ of the maximal response increases from 31 only to 33 s, while $I_{\max}$ increases from 19.7 event to 38 $\mathrm{nA/cm^2}$ at $V_{\max}$ = 0.75 μM ($\alpha^2 = 2$) and d_2 = 10 μm ($\hat{d}_2 = 0.1$).

Figure 2 also shows that the biosensor response noticeably depends on the thickness d_2 of the dialysis membrane. An increase in d_2 prolongs the time of the maximal current. As one can see in figure 2 that the maximal current decreases when the thickness d_2 of the dialysis membrane increases. FIA biosensing systems have been already investigated by using mathematical models at zero thickness of the dialysis membrane (Baronas et al. 2002, 2011). Figure 2 visually substantiates the importance of the dialysis membrane.

5. RESULTS AND DISCUSSION

Using the numerical simulation, the biosensor action was analysed with a special emphasis to the conditions at which the biosensor sensitivity can be increased and the calibration curve can be prolonged by changing the biosensor geometry (especially the thickness of the dialysis membrane), the injection duration, and the catalytic activity of the enzyme. In order to investigate the influence of the model parameters on the half maximal effective concentration C_{50} of the substrate the simulation was performed at wide ranges of the values of the thickness d_2 of the dialysis membrane, the diffusion module α^2 and the injection time T_F.

The dimensionless half maximal effective concentration $\hat{C}_{50}$ expresses the relative prolongation (in times) of the calibration curve in comparison with the theoretical Michaelis constant K_M. For the biosensor of a concrete configuration, the concentration C_{50} as well as the apparent Michaelis-Menten constant can be rather easily calculated by multiple simulation of the maximal response changing the substrate concentration S_0 (Baronas et al. 2010, 2011).

Figure 3 shows the dependence of the dimensionless half maximal effective concentration $\hat{C}_{50}$ on the thickness d_2 of the dialysis membrane. The the concentration C_{50} was calculated and then normalized with respect to the Michaelis constant K_M at three values of the diffusion module α^2: 0.1 (curves 1 and 2), 1 (3, 4) and 10 (5, 6), and two practically extreme values of the injection time T_F: 1 (1, 3, 5) and 10 s (2, 4, 6). At all these values of α^2 and T_F, the simulations were performed by changing the thickness d_2 from 5 μm ($\hat{d}_2 = 0.025$) to 40 μm ($\hat{d}_2 = 0.2$).

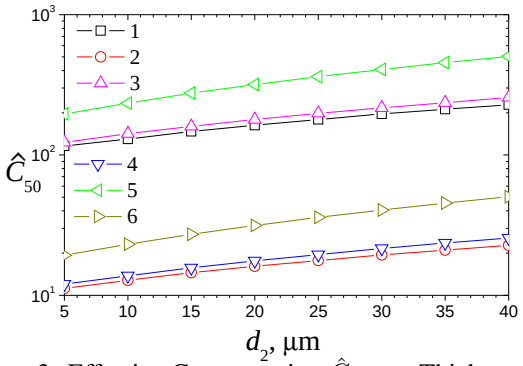

Figure 3: Effective Concentration $\hat{C}_{50}$ vs. Thickness d_2 of the Dialysis Membrane; α^2: 0.1 (1, 2), 1 (3, 4), 10 (5, 6), T_F: 1 (1, 3, 5), 10 s (2, 4, 6)

One can see in figure 3, that the dimensionless half maximal effective concentration $\hat{C}_{50}$ (as well as the corresponding dimensional concentration C_{50}) is a monotonous increasing function of the thickness d_2 of the dialysis membrane. An increase in the thickness d_2 noticeably prologs the linear part of the calibration curve of the biosensor. This can be explained by increasing an addition external diffusion limitation caused by the increasing the thickness of the membrane (Gutfreund 1995; Scheller and Schubert 1992; Ivanauskas et al. 2008; Stikoniene et al. 2010). This figure also shows a significant dependence of C_{50} on the diffusion module α^2 when $\alpha^2 \leq 1$.

To properly investigate the impact of the injection time T_F on the length of the linear part of the calibration curve, the dimensionless half maximal effective concentration $\hat{C}_{50}$ was also calculated by changing T_F from 0.5 up to 10 s. Values of $\hat{C}_{50}$ were calculated at three values of the diffusion module α^2 (0.1, 1 and 10) and two values of the thickness d_2 (10 and 20 μm) of the dialysis membrane. The calculation results are depicted in figure 4.

Figure 4 shows that $\hat{C}_{50}$ approximately exponentially increases with decreasing the injection time T_F. The calibration curve of the biosensor can be prolonged by more than an order of magnitude only by a decrease in the injection time T_F. This impact of T_F on the biosensor sensitivity only slightly depends the thickness d_2 of the dialysis membrane and the diffusion module α^2. A similar effect was also noticed when modeling a

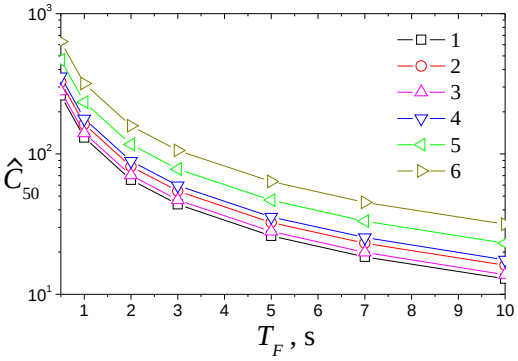

Figure 4: Effective Concentration $\hat{C}_{50}$ vs. Injection Time T_F; α^2: 0.1 (1, 2), 1 (3, 4), 10 (5, 6), d_2: 10 (1, 3, 5), 20 μm(2, 4, 6)

more simple biosensor containing no dialysis membrane (Baronas et al. 2011).

One can also see in figure 4 that the effective concentration $\hat{C}_{50}$ is noticeably higher at greater values of the diffusion module α^2 than at lower ones.

To investigate the impact of the diffusion module α^2 on the effective concentration the biosensor responses were simulated at a wide range of values of α^2. The simulation results are presented in figure 5. The effective concentration $\hat{C}_{50}$ was calculated at two values of the thickness d_2 (10 and 20 μm) of the dialysis membrane and two values of the injection time T_F (1 and 10 s). At concrete values of d_2 and T_F, the calculations were performed by changing the maximal enzymatic rate $V_{\max}$ from 75 nM/s ($\alpha^2 = 0.1$) to 7.5 μM/s ($\alpha^2 = 10$) while keeping the all other parameters constant.

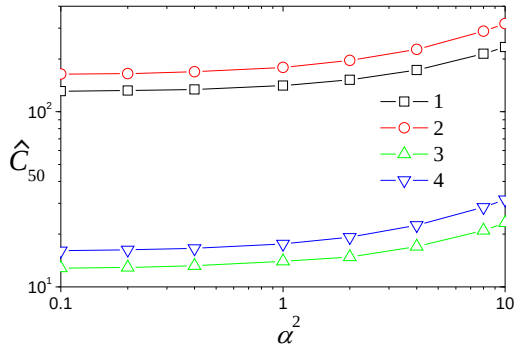

Figure 5: Effective Concentration $\hat{C}_{50}$ vs. Diffusion Module α^2; d_2: 10 (1, 3), 20 μm(2, 4), T_F: 1 (1, 2), 10 s (3, 4)

As one can see in figure 5 that the effective concentration $\hat{C}_{50}$ is a monotonous increasing function of α^2. When the enzyme kinetics predominates in the biosensor response ($\alpha^2 \ll 1$) the concentration $\hat{C}_{50}$ is approximately a constant function. In the opposite case of the biosensor operation when the biosensor response is under diffusion control ($\alpha^2 \gg 1$), the concentration $\hat{C}_{50}$ exponentially increases with an increase in the diffusion module α^2. A similar influence of the diffusion module α^2 to the linear part of the calibration curver was also noticed when modeling the corresponding biosensor with no dialysis membrane (Baronas et al. 2011).

In real applications of biosensors, the diffusion module α^2 can be controlled by changing the maximal enzyme activity $V_{\max}$ as well as the thickness d_1 of the enzyme layer. The maximal enzymatic rate $V_{\max}$ is actually a product of two parameters: the catalytic constant k_2 introduced in (1) and the total concentration of the enzyme (Gutfreund 1995; Scheller and Schubert 1992). Since, in actual applications it is usually impossible to change a value of the constant k_2, the maximal rate $V_{\max}$ as well as the diffusion module α^2 might be changed by changing the enzyme concentration in the enzyme layer.

6. CONCLUSIONS

The mathematical model (3)-(10) of an amperometric biosensor containing a dialysis membrane and utilizing the flow injection analysis can be successfully used to investigate the kinetic peculiarities of the biosensor response. The corresponding dimensionless mathematical model (15)-(21) can be applied to the numerical investigation of the impact of model parameters on the biosensor action and to optimize the biosensor configuration.

By increasing the thickness d_2 of the dialysis membrane, the half maximal effective concentration $\hat{C}_{50}$ can be increased and the linear part of the biosensor calibration curve can be prolonged several fold (see figure 3).

The half maximal effective concentration $\hat{C}_{50}$ approximately exponentially increases with decreasing the injection time T_F. The calibration curve of the biosensor can be prolonged by a few orders of magnitude by decreasing the injection time T_F (figure 4).

The half maximal effective concentration $\hat{C}_{50}$ is a monotonous increasing function of the diffusion module α^2. When the enzyme kinetics distinctly predominates in the response ($\alpha^2 \ll 1$), the $\hat{C}_{50}$ is approximately a constant function of α^2, while at $\alpha^2 \gg 1$ the concentration $\hat{C}_{50}$ exponentially increases with an increase in α^2 (figure 5).

ACKNOWLEDGMENTS

The research by R. Baronas is funded by the European Social Fund under the Global Grant measure, Project No. VP1-3.1-ŠMM-07-K-01-073/MTDS-110000-583. The authors thank participants of the seminar of Vilnius University "BioModa" for valuable discussions.

REFERENCES

Amatore, C., Oleinick, A., Svir, I., da Mota, N., and Thouin, L., 2006. Theoretical modeling and optimization of the detection performance: a new concept for electrochemical detection of proteins in microfluidic channels. *Nonlinear Analysis: Modelling and Control*, 11(4):345–365.

Baronas, D., Ivanauskas, F., and Baronas, R., 2011. Mechanisms controlling the sensitivity of amperometric biosensors

in flow injection analysis systems. *Journal of Mathematical Chemistry*, 49(8):1521–1534.

Baronas, R., Ivanauskas, F., and Kulys, J., 2002. Modelling dynamics of amperometric biosensors in batch and flow injection analysis. *Journal of Mathematical Chemistry*, 32(2):225–237.

Baronas, R., Ivanauskas, F., and Kulys, J., 2010. *Mathematical Modeling of Biosensors*. Springer, Dordrecht.

Bartlett, P. N. and Whitaker, R. G., 1987. Electrochemical imobilization of enzymes: Part 1. Theory. *Journal of Electroanalytical Chemistry*, 224(1–2):27–35.

Bisswanger, H., 2008. *Enzyme Kinetics: Principles and Methods*. Wiley-VCH, Weinheim (Germany), 2 edition.

Britz, D., 2005. *Digital Simulation in Electrochemistry*. Springer, Berlin, 3 edition.

Britz, D., Baronas, R., Gaidamauskaitė, E., and Ivanauskas, F., 2009. Further comparisons of finite difference schemes for computational modelling of biosensors. *Nonlinear Analysis: Modelling and Control*, 14(4):419–433.

Cervini, P. and Cavalheiro, É. T. G., 2008. Determination of paracetamol at a graphite-polyurethane composite electrode as an amperometric flow detector. *Journal of the Brazilian Chemical Society*, 19(5):836–841.

Gough, D. and Leypoldt, J., 1979. Membrane-covered, rotated disk electrode. *Analytical Chemistry*, 51:439–444.

Gruhl, F. J., Rapp, B. E., and Länge, K., 2011. Biosensors for diagnostic applications. In *Advances in Biochemical Engineering Biotechnology*, pages 1–34. Springer Berlin Heidelberg.

Gutfreund, H., 1995. *Kinetics for the Life Sciences*. Cambridge University Press, Cambridge.

Hernandez, P., Rodriguez, J. A., Galan, C. A., Castrillejo, Y., and Barrado, E., 2013. Amperometric flow system for blood glucose determination using an immobilized enzyme magnetic reactor. *Biosensors and Bioelectronics*, 41(9–12):244–248.

Ivanauskas, F., Kaunietis, I., Laurinavičius, V., Razumienė, J., and Šimkus, R., 2008. Apparent michaelis constant of the enzyme modified porous electrode. *Journal of Mathematical Chemistry*, 43(4):1516–1526.

Kernevez, J. P., 1980. *Enzyme Mathematics*, volume 10 of *Studies in Mathematics and its Applications*. Elsevier Science, Amsterdam.

Kulys, J., 1981. The development of new analytical systems based on biocatalysts. *Analytical Letters*, 14(6), 377–397.

Lyons, M. E. G., 2009. Transport and kinetics at carbon nanotube - redox enzyme composite modified electrode biosensors. *International Journal of Electrochemical Science*, 4(1):77–103.

Mello, L. and Kubota, L., 2002. Review of the use of biosensors as analytical tools in the food and drink industries. *Food Chemistry*, 77(2):237–256.

Nenkova, R., Atanasova, R., Ivanova, D., and Godjevargova, T., 2010. Flow injection analysis for amperometric detection of glucose with immobilized enzyme reactor. *Biotechnology & Biotechnological Equipment*, 24(3):1986–1992.

Press, W., Teukolsky, S., Vetterling, W., and Flannery, B., 1992. *Numerical Recipes in C: The Art of Scientific Computing*. Cambridge University Press, Cambridge (UK), 2 edition.

Prieto-Simon, B., Campas, M., Andreescu, S., and Marty, J.-L., 2006. Trends in flow-based biosensing systems for pesticide assessment. *Sensors*, 6(10):1161–1186.

Ruzicka, J. and Hansen, E., 1988. *Flow Injection Analysis*. Wiley, New York.

Scheller, F. W. and Schubert, F., 1992. *Biosensors*. Elsevier Science, Amsterdam.

Schulmeister, T., 1990. Mathematical modelling of the dynamic behaviour of amperometric enzyme electrodes. *Selective Electrode Reviews*, 12:203–260.

Segel, L. A. and Slemrod, M., 1989. The quasi-steady-state assumption: a case study in perturbation. *SIAM Review*, 31(3):446–477.

Simelevicius, D., Baronas, R., and Kulys, J., 2012. Modelling of amperometric biosensor used for synergistic substrates determination. *Sensors*, 12(4):4897–4917.

Stikoniene, O., Ivanauskas, F., and Laurinavicius, V., 2010. The influence of external factors on the operational stability of the biosensor response. *Talanta*, 81(4–5):1245–1249.

Turner, A. P. F., Karube, I., and Wilson, G. S., editors, 1990. *Biosensors: Fundamentals and Applications*. Oxford University Press, Oxford.

van Stroe-Blezen, S., Everaerts, F. M., Janssen, L. J. J., and Tacken, R. A., 1993. Diffusion coefficients of oxygen, hydrogen peroxide, and glucose in a hydrogel. *Analytica Chimica Acta*, 273:553–560.

Viswanathan, S., Radecka, H., and Radecki, J., 2009. Electrochemical biosensors for food analysis. *Monatshefte Fur Chemie*, 140(8):891–899.

Wollenberger, U., Lisdat, F., and Scheller, F. W., 1997. *Frontiers in Biosensorics 2, Practical Applications*. Birkhauser Verlag, Basel.

Zhang, S., Zhao, H., and John, R., 2001. Development of a quantitative relationship between inhibition percentage and both incubation time and inhibitor concentration for inhibition biosensors–theoretical and practical considerations. *Biosensors and Bioelectronics*, 16(9–12):1119–1126.

AUTHORS BIOGRAPHY

Romas Baronas was born in 1959 in Kybartai, Lithuania. He enrolled at the Vilnius University, where he studied applied mathematics and received his Ph.D. degree. Now he is a professor and serves as the head of the department of Software Engineering at Vilnius University. His research interests are in database systems, software engineering, and computational modeling of nonlinear phenomena in life sciences.

Darius Baronas is a PhD student at Institute of Mathematics and Informatics of Vilnius University. He graduated that University in 2007. His research interests are focused on computational modeling and optimization of biochemical processes.